Available online at www.sciencedirect.com
ScienceDirect
Biosensors and Bioelectronics 23 (2007) 135–139
BIOSENSORS & BIOELECTRONICS
www.elsevier.com/locate/bios

Short communication

A novel amperometric biosensor based on ZnO:Co nanoclusters for biosensing glucose

Z.W. Zhao [a,e,*], X.J. Chen [b], B.K. Tay [a], J.S. Chen [c,d,**], Z.J. Han [a], K.A. Khor [b]

[a] School of Electrical and Electronic Engineering, Nanyang Technological University, Singapore 639798, Singapore
[b] School of Mechanical & Aerospace Engineering, Nanyang Technological University, Singapore 639798, Singapore
[c] Department of Materials Science and Engineering, National University of Singapore, Singapore 119260, Singapore
[d] Data Storage Institute, DSI Building, 5 Engineering Drive 1, Singapore 117608, Singapore
[e] School of Electronic Science and Engineering, Southeast University, Nanjing, 210096, China

Received 4 December 2006; received in revised form 26 February 2007; accepted 19 March 2007
Available online 30 March 2007

Abstract

ZnO:Co nanoclusters were synthesized by nanocluster-beam deposition with averaged particle size of 5 nm and porous structure, which were for the first time adopted to construct a novel amperometric glucose biosensor. Glucose oxidase was immobilized into the ZnO:Co nanocluster-assembled thin film through Nafion-assisted cross-linking technique. Due to the high specific active sites and high electrocatalytic activity of the ZnO:Co nanoclusters, the constructed glucose biosensor showed a high sensitivity of 13.3 μA/mA cm^2. The low detection limit was estimated to be 20 μM (S/N = 3) and the apparent Michaelis–Menten constant was found to be 21 mM, indicating the high affinity of the enzyme on ZnO:Co nanoclusters to glucose. The results show that the ZnO:Co nanocluster-assembled thin films with nanoporous structure and nanocrystallites have potential applications as platforms to immobilize enzyme in biosensors.

Keywords: ZnO; Nanoclusters; Glucose biosensor; Cross-linking

1. Introduction

Glucose biosensor, as one of the most popular biosensors, has been intensively investigated due to its importance in clinics, environment and food industry. Glucose oxidase (GOx) is often used as the enzyme in glucose amperometric biosensors to catalyze the oxidation of glucose and the reaction could be detected in a form of current at the electrode. Since the first glucose biosensor in 1962 (Clark and Lyons, 1962), extensive efforts have been made on the improvement of the performance and stability of enzyme electrodes, where modified electrodes with various configurations and the performance of the constructed biosensors have attracted great interests. Recent biosensor development is based on combing the properties of biologically active substances with those of inorganic nanocrystalline materials. These inorganic materials with nanostructure could provide large surface to volume ratio and the increased surface activity, making their unique advantages over other conventional materials for enzymatic immobilization and signal transduction. They could keep activity of enzyme due to the desirable microenvironment, and enhance the direct electron transfer between the enzyme's active sites and the electrode (Zhang et al., 2004).

Up to now, many inorganic nanomaterials, such as gold nanoparticles and nanoclusters (Zhang et al., 2005; S. Zhao et al., 2006; Bharathi et al., 2001), Au/polyaniline nanocomposite (Xian et al., 2006), carbon nanotube (Liu et al., 2005), nanocrystalline diamond (Zhao et al., 2006), calcium carbonate nanoparticles (Shan et al., 2007) and Ag dendritic nanostructures (Wen et al., 2006), have been studied as signal transducers and platforms for the enzyme immobilization in biosensors. ZnO as a wide band gap (3.37 eV) semiconductor plays an important role in optics, optoelectronics, sensors, and actuators due to its semiconducting, piezoelectric, and pyroelectric properties (Norton et al., 2004; Sun and Kwok, 1999). Nanostructured ZnO not only possesses high surface area, nontoxicity, good bio-

* Corresponding author. Tel.: +86 25 83792250; fax: +86 25 83794756.
** Corresponding author at: Department of Materials Science and Engineering, National University of Singapore, Singapore 119260, Singapore. Tel.: +65 65167574; fax: +65 67763604.
E-mail addresses: zzwsg@hotmail.com (Z.W. Zhao), msecj@nus.edu.sg (J.S. Chen).

0956-5663/$ – see front matter © 2007 Elsevier B.V. All rights reserved.
doi:10.1016/j.bios.2007.03.014

compatibility and chemical stability, but also shows biomimetic and high electron communication features (Tian et al., 2002; Sberveglieri et al., 1995; Rodriguez et al., 2000), making it great potential applications in biosensors. Zhang et al. (2004) have reported a reagentless uric acid biosensor based on ZnO nanorodes. Recently, GOx was immobilized on ZnO nanocombs and nanorods to construct an amperometric biosensor for glucose biosensing (Wang et al., 2006; Wei et al., 2006), showing a sensitivity of 15–23 $\mu A/mA\,cm^2$.

Nanoclusters, as a bridge between molecules and bulk materials, are aggregates of a small and finite number of atoms or molecules, which could be ranged from several atoms up to large nanoclusters made up of several tens of thousands of atoms. The nanocluster-assembled thin films/materials have attracted increasing interests due to novel properties and technological applications. In addition to their small nanocrystallites in several nanometers, ZnO-based nanoclusters possess nanoporous network structure, making them different from previous ZnO nanorods, nanocombs, nanowires and other low dimensional nanostructures. In our group, the unique optical and magnetic properties of the ZnO-based nanoclusters (Zhao et al., 2007) have been demonstrated. Cobalt shows high electrocatalytic activity for the oxygen reduction and low detecting potential for hydrogen peroxide, posing it great potential application in fuel cell and biosensor development (Cataldi et al., 1995). In this work, ZnO:Co nanoclusters (doping 2% Co in ZnO) with small average size of 5 nm and density as low as one-third of ZnO bulk materials were developed and employed for the first time to construct a novel amperometric glucose biosensor by taking the advantages of the high electrocatalytic activity of ZnO and cobalt and the high specific surface area of the nanocluster structure.

2. Experiments

2.1. Reagents and material

The glucose oxidase (EC1.1.3.4, from *Aspergillus niger*, 200 units/mg), β-D-(+)-glucose, 25% glutaraldehyde and bovine serum albumin (BSA) were obtained from Sigma–Aldrich and used without further purification. The buffer solutions were prepared from 0.08 M K_2HPO_4 and 0.02 M KH_2PO_4 (99.9%, Sigma–Aldrich). All the solutions were prepared with a Millipore Q water (resistance: $\sim$18.0 $M\Omega\,cm^{-1}$). Glucose stock solutions were prepared and kept overnight at room temperature before use to allow mutarotation. The poly(ethylene terephthalate) (PET) plate used as a substrate for electrode was purchased from *Goodfellow* with a thickness of 200 μm.

2.2. Synthesis of nanocluster-assembled ZnO:Co thin films

ZnO:Co nanoclusters, produced by a magnetron sputtering gas aggregation source, were obtained by a nanocluster-beam deposition system as described in the literature (Chen et al., 2005; Zhao et al., 2005). The growth region was cooled with liquid nitrogen and kept the temperature at 170 K. A 2 in. metal target consisting of 98% Zn and 2% Co was used and DC sputtering power was 130 W. Ar, He and O_2 gases with a corresponding total pressure of 0.75 Torr were introduced into the system, and ZnO:Co nanoclusters were thus formed and further deposited onto the substrates.

2.3. Fabrication of PET/Ti/Au/ZnO:Co electrode

Metal Ti thin layer on PET plate was implanted by plasma immersion ion implantation technology at 12 keV with a dose of 10^9 ions/cm^3, where the Ti ions were obtained from the plasma generated by a filtered cathodic vacuum arc source with an arc current of 90 A. The Ti layer thickness including the penetration depth in PET was about 20 nm. After that, Au layer with thickness of 30 nm was deposited on Ti-implanted PET substrate by DC magnetron sputtering with power of 20 W at room temperature. This process makes the Au layer well adhesive to Ti/PET substrate with excellent conductivity (20 Ω/sq). The obtained PET/Ti/Au electrode was then loaded to the chamber of nanocluster-beam system for the deposition of ZnO:Co nanoclusters. The thickness of nanocluster-assembled thin film was around 300 nm.

2.4. Immobilization of glucose oxidase on PET/Ti/Au/ZnO:Co electrode

GOx solution was prepared by dissolving 30.0 mg GOx and 20 mg BSA in 1.0 mL phosphate buffer solution (PB, 0.1 M, pH 7.4). Cross-linking method was employed to immobilize glucose oxidase on PET/Ti/Au/ZnO:Co electrode. In brief, 100 μL above GOx solution, 50 μL 2.5% glutaraldehyde and 50 μL 0.5% Nafion solution were mixed thoroughly. Subsequently, 4 μL above mixture solution was applied onto the PET/Ti/Au/ZnO:Co electrode surface and allowed to dry in air at room temperature. Finally, 4 μL 0.5% Nafion was further coated on the enzyme electrode to eliminate the possible fouling and prevent the leaching of the enzyme. The enzyme electrodes were kept dry in refrigerator at 4 °C when not in use.

2.5. Characterization and amperometric measurement

Surface morphology of ZnO:Co nanoclusters was characterized using atomic force microscopy (AFM) in tapping mode (Dimension 3000 scanning probe microscope from Digital Instrument). Transmission electron microscopy (TEM, JEOL 2010) operated at 200 keV was used for the examination of microstructure of the obtained ZnO:Co nanoclusters on carbon coated copper gird. X-ray photoelectronic spectroscopy (XPS) was used to study the chemical states of the film. All the amperometric measurements of the enzyme electrodes were carried out in an Autolab electrochemical analyzer (Autolab/PGSTAT30, ECO CHEMIE, Netherlands). A conventional three-electrode configuration was employed consisting of a fabricated PET/Ti/Au/ZnO:Co electrode as the working electrode, a platinum foil as the counter electrode, and a Ag/AgCl, KCl (3 M) electrode as the reference electrode. The amperometric response measurements were carried out in phosphate buffer solution (PB, pH 7.4) at applied potential of 0.8 V versus Ag/AgCl reference

electrode under stirring. The measurement temperature was kept at room temperature (about 24 ± 2 °C).

3. Results and discussion

Fig. 1 shows AFM image of ZnO:Co nanoclusters-assembled thin film scanned in an area of 1 μm × 1 μm. Obviously, the thin film is composed of aggregates of spherical primary particles. These aggregates pack together to form thin film but with interparticle nanopores and confirmed by the sharp contrast in the image. The inset obtained by TEM in Fig. 1 shows a typical high-resolution image of one ZnO:Co nanocluster, where the nanocluster is in single crystallite state with the clear lattice fringes. These nanoclusters are generally spherical with an average size of 5 nm. The electron diffraction pattern (not shown) exhibits several separated rings and are identified as being consistent with wurtzite ZnO structure. Using low-energy nanocluster-beam deposition, the nanoclusters will stick on the substrates without scattering and fragmentation. The nucleation and film growth is by random stacking of supported particles when considering the limited diffusion and coalescence effects of large supported nanoclusters. The structure of the nanocluster-assembled thin films/materials differ from those of amorphous and crystalline materials in that the short range order in them is controlled by the grain size, while the long range order does not exist due to random stacking of nano-grains. Thus, the obtained cluster-assembled nanomaterials are highly nanoporous in network with the density just as one-third of ZnO bulk density, which provide high reactive surface area for mass enzyme loading and the good microenvironment favoring the keeping of enzyme activity.

XPS is used to characterize the chemical state of the elements (e.g. Zn, O, Co) of the nanoclusters. It is found that in addition to the strong peaks from O and Zn ions, Co signal is also observed, but with weak intensity due to the low concentration (not shown). The binding energies of Zn $2p_{1/2}$ at 1045 eV and Zn $2p_{3/2}$ at 1021.7 eV are coincided with those of the standards for bulk ZnO, indicating the full oxidation of Zn ions in the nanoclusters. From the narrow scan of Co 2p core-level photoemission spectrum, the binding energy of Co $2p_{3/2}$ is located at 780.9 eV, while the Co $2p_{1/2}$ peak is at 796.6 eV. The large chemical shift of 15.6 eV between Co $2p_{3/2}$ and Co $2p_{1/2}$ compared to that of pure Co metal (15.05 eV) indicates that Co ions are preferred in +2 oxidation state and further supported by the observed two shake-up satellites on the higher binding energy. Hence, from the characterization it could be concluded that both Zn and cobalt are in the +2 oxidation state.

In order to understand the potential window for the glucose detection, the PET/Ti/Au/ZnO:Co/GOx enzyme electrode was characterized by cyclic voltammetry between the potentials of −0.2 and 0.8 V with respective to the Ag/AgCl reference electrode. Fig. 2 shows the cyclic voltammograms of the PET/Ti/Au/ZnO:Co/GOx electrode in stirred 0.1 M PB with and without 2 mM glucose. In the absence of glucose, no obvious redox peaks were observed between the potential scanning ranges of −0.2 to 0.8 V. The currents observed at potentials below −0.1 V and above 0.5 V correspond to the evolution of hydrogen peroxide and oxygen on the enzyme electrode surface, respectively. With the addition of 2 mM glucose into the PB, a sharp current increase at potential above 0.3 V was observed, suggesting strong amperometric response of the PET/Ti/Au/ZnO:Co/GOx electrode to glucose. In addition, a broad shoulder appeared at potential around 0.55 V in PB solution with 2 mM glucose. The pattern of the cyclic voltammogram of the enzyme electrode in glucose solution is similar to that in H_2O_2 solution, implying that the current increase in the presence of glucose is attributed to the oxidation of H_2O_2

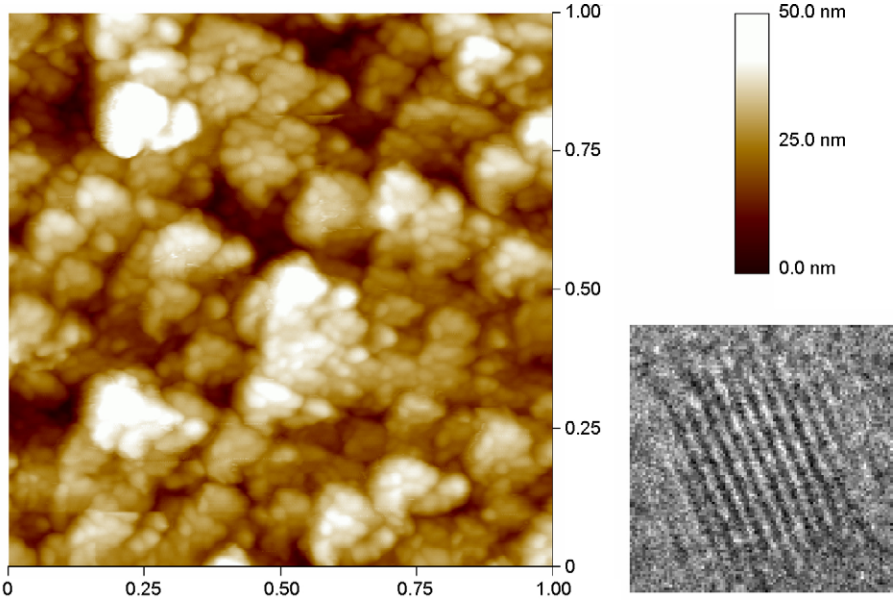

Fig. 1. AFM image of the ZnO:Co nanoclusters-assembled thin film. The inset (right bottom) shows a high-resolution TEM of a ZnO:Co nanocluster with clear lattice fringes.

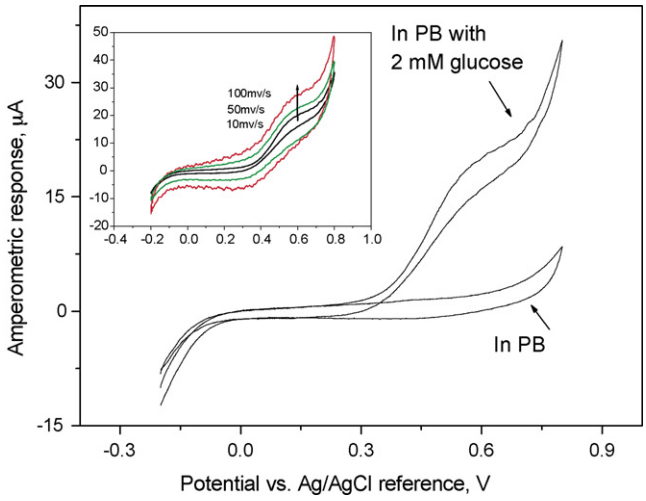

Fig. 2. Cyclic voltammograms of PET/Ti/Au/ZnO:Co/GOx electrode at a scanning rate of 10 mV/s in 0.1 M PB (pH 7.4) in the absence and presence of 2 mM glucose. The inset shows the cyclic voltammograms of the electrode as a function of scanning rate.

generated by the enzymatic reactions. As shown in the insert of Fig. 2, the peak current at potential of 0.55 V is proportional to the scanning rate, which shows a typical charge-transfer controlled electrochemical behavior, indicating the fast diffusion of H_2O_2 through the enzyme film to the ZnO:Co electrocatalyst surface.

The performance of the biosensor was evaluated by testing the PET/Ti/Au/ZnO:Co/GOx electrode in glucose with increased concentration. After the background current in PB reached stable, 0.2 mM glucose solution was successively injected into the stirring PB and the current was recorded continuously. Fig. 3(a) shows the steady state amperometric response of the PET/Ti/Au/ZnO:Co/GOx to the successive step additions of glucose into the stirring PB. A subsequent addition of glucose to the solution provoked a remarkable increase in the oxidation current. When an aliquot of glucose was added into the buffer solution, the oxidation current rose steeply to reach a stable value. The response time was around 8 s for the enzyme electrode to reach 95% steady state current. The calibration curve (Fig. 3(b)) with linear range spans the concentration of glucose from 0 to 4 mM, which is similar to those observed in ZnO nanocomb and nanorod constructed biosensors (Wang et al., 2006; Wei et al., 2006). This kind of biosensor has a low detection limit of 20 μM (be estimated based on the signal-to-noise characteristics of these data (S/N = 3)) and a high sensitivity of 13.3 μA/mM cm^2. The high sensitivity of the enzyme electrode can be attributed to the excellent adsorption ability, high electrocatalytic activity and good biocompatibility of the ZnO:Co nanoclusters. The apparent Michaelis–Menten constant (K_M^{app}), which gives an indication of the enzyme–substrate kinetics for the glucose biosensor, can be calculated from the well-known Lineweaver–Burk equation. The derived K_M^{app} was 21 mM, which was lower than 27 mM for native GOx in solution (Rogers and Brandt, 1971), 33 mM at the GOx–DMFc–CPE (Amine et al., 1993) and 25.3 mM at the GOx–polypyrrole (Vidal et al., 1998), indicating of a high affinity to glucose of the GOx in the film. The storage stability

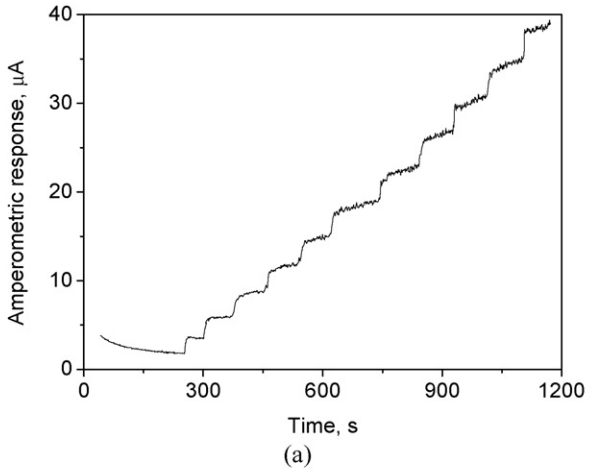

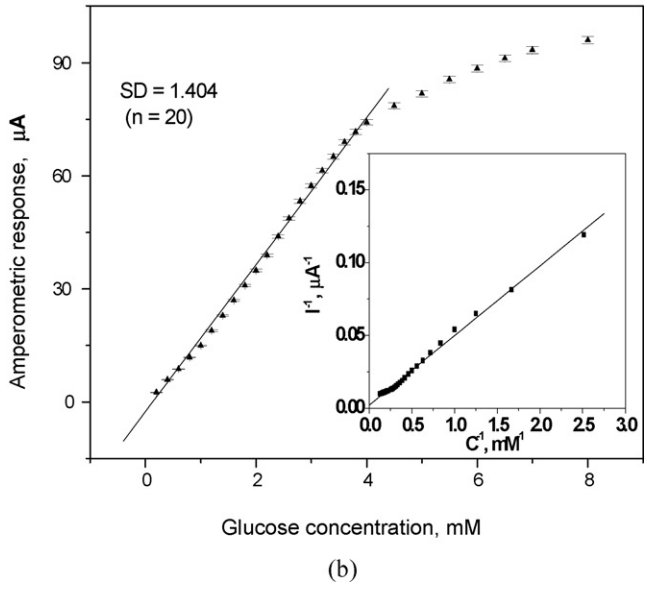

Fig. 3. (a) Amperometric responses of PET/Ti/Au/ZnO:Co/GOx electrode with the successive addition of 0.2 mM glucose to the 0.1 M PB (pH 7.4) buffer under stirring; (b) linear calibration curve of the enzyme electrode.

of the biosensor was tested over 2 weeks and less than a 10% decrease in the response to 2 mM glucose was found over this period.

4. Conclusions

A novel amperometric glucose biosensor was constructed by using ZnO:Co nanoclusters as platform for the glucose oxidase immobilization. With the combination of the large specific surface area and high electrocatalytic activity of the ZnO:Co nanoclusters, the developed biosensor has a high sensitivity of 13.3 μA/mM cm^2 for glucose detection and low detection limit of 20 μM (S/N = 3). The interference of some species, such as uric acid and ascorbic acid, cannot be completely removed for the biosensor at the operating potential. Thus, the possible application of this kind of biosensor may be focused on environmental and industrial monitoring.

Acknowledgement

Dr. Chen Xiaojun would also like to appreciate the financial support from Singapore Millennium Foundation for the project.

References

Amine, A., Kauffmann, J.M., Guilbault, G.G., 1993. Anal. Lett. 26, 1281–1299.
Bharathi, S., Nogami, M., Lev, O., 2001. Langmuir 17, 2602–2609.
Cataldi, T.R.I., Guerrieri, A., Casella, I.G., Desimoni, E., 1995. Electroanalysis 7, 305–311.
Chen, J.S., Tan, C.Y., Chow, S.Y., Liu, B., Chow, G.M., 2005. J. Appl. Phys. 98, 064306–064309.
Clark, L.C., Lyons, C., 1962. Ann. N. Y. Acad. Sci. 102, 29–45.
Liu, Y., Wang, M., Zhao, F., Xu, Z., Dong, S., 2005. Biosens. Bioelectron. 21, 984–988.
Norton, D.P., Heo, Y.W., Ivill, M.P., Pearton, S.J., Chisholm, M.F., Steiner, T., 2004. Mater. Today 7, 34–40.
Rodriguez, J.A., Jirsak, T., Dvorak, J., Sambasivan, S., Fischer, D., 2000. J. Phys. Chem. B 104, 319–328.
Rogers, M.J., Brandt, K.G., 1971. Biochem. 10, 4624–4630.
Sberveglieri, G., Groppelli, S., Nelli, P., Tintinelli, A., Giunta, G., 1995. Sens. Actuators B 25, 588–590.
Shan, D., Zhu, M., Xue, H., Cosnier, S., 2007. Biosens. Bioelectron. 22, 1612–1617.
Sun, X.W., Kwok, H.S., 1999. J. Appl. Phys. 86, 408–411.
Tian, Z.R.R., Voigt, J.A., Liu, J., Mckenzie, B., Mcdermott, M.J., 2002. J. Am. Chem. Soc. 124, 12954–12955.
Vidal, J.C., Garcia, E., Castillo, J.R., 1998. Biosens. Bioelectron. 13, 371–382.
Wang, J.X., Sun, X.W., Wei, A., Lei, Y., Cai, X.P., Li, C.M., Dong, Z.L., 2006. Appl. Phys. Lett. 88, 233106–233108.
Wei, A., Sun, X.W., Wang, J.X., Lei, Y., Cai, X.P., Li, C.M., Dong, Z.L., 2006. Appl. Phys. Lett. 89, 123902–123905.
Wen, X.G., Xie, Y.T., Mak, M.W.C., Cheung, K.Y., Li, X.Y., Renneberg, R., Yang, S.H., 2006. Langmuir 22, 4836–4842.
Xian, Y., Hu, Y., Liu, F., Xian, Y., Wang, H., Jin, L., 2006. Biosens. Bioelectron. 21, 1996–2000.
Zhang, F.F., Wang, X.L., Ai, S.Y., Sun, Z.D., Wan, Q., Zhu, Z.Q., Xian, Y.Z., Jin, L.T., Yamamoto, K., 2004. Anal. Chim. Acta 519, 155–160.
Zhang, S., Wang, N., Niu, Y., Sun, C., 2005. Sens. Actuators B 109, 367–374.
Zhao, S., Zhang, K., Bai, Y., Yang, W.W., Sun, C., 2006. Bioelectrochemistry 69, 158–163.
Zhao, W., Xu, J.J., Qiu, Q.Q., Chen, H.Y., 2006. Biosens. Bioelectron. 22, 649–655.
Zhao, Z.W., Tay, B.K., Chen, J.S., Hu, J.F., Sun, X.W., Tan, S.T., 2005. Appl. Phys. Lett. 87, 251912–251924.
Zhao, Z.W., Tay, B.K., Chen, J.S., Hu, J.F., Lim, B.C., 2007. Appl. Phys. Lett. 90, 152502–152504.